

Contribution from the Department of Chemistry,  
Texas A&M University, College Station, Texas 77843-3255

## Synthesis, Separation, and Equilibrium Characterization of Racemic and Meso Forms of a New Multidentate Ligand:

### *N,N'*-Trimethylenebis[2-(2-hydroxy-3,5-dimethylphenyl)glycine], TMPHPG

Christopher J. Bannochie<sup>†</sup> and Arthur E. Martell\*

Received July 12, 1990

The racemic and meso forms of the EHPG analogue *N,N'*-trimethylenebis[2-(2-hydroxy-3,5-dimethylphenyl)glycine], TMPHPG, have been separated by exploiting a stability difference in their iron(III) complexes. Assignment of the two diastereomers has been made on the basis of the <sup>1</sup>H NMR spectra of their respective gallium(III) complexes. Ligand protonation and metal ion equilibria with iron(III), gallium(III), and indium(III) have been measured. The increased separation of the two chiral centers relative to that in EHPG (*N,N'*-ethylenebis[2-(2-hydroxy-3,5-dimethylphenyl)glycine]) was found to reduce the stability differences between the diastereomeric complexes. The increased phenol basicity, in combination with the longer diamine bridge length, significantly reduced the effectiveness of these ligands in the binding of indium(III). Calculated pM values indicate that while in vivo exchange of iron(III) and gallium(III) from the complexes to transferrin would be unlikely, indium(III) exchange would be expected.

### Introduction

In the course of our work to produce new, more lipophilic multidentate ligands for use in radiopharmaceuticals (<sup>68</sup>Ga(III), <sup>111</sup>In(III)) and contrast agents for magnetic resonance imaging (Fe(III)), we have prepared and characterized a new, more lipophilic derivative of the multidentate ligand *N,N'*-ethylenebis[2-(*o*-hydroxyphenyl)glycine] (EHPG). Like EHPG,<sup>1</sup> *N,N'*-trimethylenebis[2-(2-hydroxy-3,5-dimethylphenyl)glycine] (TMPHPG), shown in Figure 1, exists in two diastereomeric forms consisting of a racemic mixture and a meso isomer. Recent work has shown that the two diastereomers of EHPG display stereospecific behavior in vivo when complexed with iron(III), gallium(III), and indium(III).<sup>2</sup> The racemic and meso forms of TMPHPG have been separated in order to evaluate their respective affinities for these trivalent metal ions. High affinity and thermodynamic stability are essential for medical applications to avoid exchange in vivo of the metal ion with naturally occurring complexing agents such as transferrin and ferritin.

### Experimental Section

NMR spectra were recorded on Varian XL-200 (dual probe), XL-400 (multiple probe), and Gemini-300 spectrophotometers. FAB analyses were obtained on a VG Analytical 70S high-resolution double-focusing magnetic sector mass spectrometer with attached VG Analytical 11/250J data system and a 3-nitrobenzyl alcohol matrix. Optical absorption spectra were measured with a Perkin-Elmer Model 553 fast-scan spectrophotometer with spectrally matched quartz cells of path length 1.000 ± 0.001 cm. Elemental analyses were performed by Galbraith Laboratories, Knoxville, TN.

**Materials.** TMPHPG was synthesized as described below. The starting materials 1,3-diaminopropane, glyoxylic acid, and 2,4-dimethylphenol were obtained from Aldrich Chemical Co. Reagent grade iron(III) chloride was obtained from Fisher Scientific Co. and used without further purification. Gallium(III) chloride (99.99+%) and indium(III) chloride (99.99+%) were obtained from Aldrich Chemical Co. Carbonate-free ampules of Dilut-It KOH were obtained from J. T. Baker Chemical Co. All aqueous solutions were prepared with CO<sub>2</sub>-free, doubly distilled water. After dilution, the KOH was standardized by titration of potassium hydrogen phthalate to a phenolphthalein end point. This standard KOH titrant was then used to standardize an aqueous solution of HCl. Iron(III) solutions were standardized according to the methods of Schwarzenbach and Flaschka,<sup>3</sup> while solutions of gallium(III) and indium(III) were standardized by ion-exchange chromatography using Dowex 50W-X8 cation-exchange resin (20–50 mesh), followed by titration of the free acid liberated.

**TMPHPG Synthesis.** Glyoxylic acid (50%) (59.2 g, 0.4 mol) was dissolved in distilled water (170 mL). While cooling in an ice bath, the solution was brought to pH 4.0 with 50% aqueous NaOH. To this solution was added 1,3-diaminopropane (15.0 g, 0.2 mol). HCl (2.0 M) was used to adjust the solution to pH 9.95. After the addition of 100 mL

of methanol the solution was brought to reflux at 85 °C for 30 min. 2,4-Dimethylphenol (50.4 g, 0.4 mol) was dissolved in methanol (100 mL) and added dropwise over a 45-min period to the refluxing solution. Following addition of the phenol, the solution was refluxed at 81 °C for an additional 12 h. After cooling, the reaction solution was extracted with three 60-mL portions of diethyl ether to remove unreacted phenol. The aqueous phase was placed on a rotary evaporator in order to remove traces of ether and as much methanol as possible. Following adjustment to pH 5.0 with 2.0 M HCl, a precipitate formed, which was collected by vacuum filtration and washed repeatedly with distilled water and acetone until free of yellow color. The nearly white ligand was dried over P<sub>2</sub>O<sub>5</sub> in a vacuum desiccator. Yield: 5.0 g, 5.8%. Anal. Calcd (found) for C<sub>23</sub>H<sub>30</sub>N<sub>2</sub>O<sub>6</sub>·<sup>3</sup>/<sub>4</sub>H<sub>2</sub>O: C, 62.22 (61.88); H, 7.15 (7.10); N, 6.31 (6.39); O, 24.32 (24.56). <sup>1</sup>H NMR (200 MHz, D<sub>2</sub>O): δ 1.80 (m, 2 H), 2.20 (s, 6 H), 2.63 (m, 4 H), 4.30 (s, 2 H) variable (see Results), 6.83 (s, 2 H), 6.95 (s, 2 H). FAB: *m/e* 431 ((M + H)<sup>+</sup>).

**Separation of TMPHPG Diastereomers.** TMPHPG (2.73 g, 6.1 mmol) was suspended in absolute ethanol (30 mL) along with 1.6 equiv of NaHCO<sub>3</sub> (0.85 g). To the refluxing slurry of ligand was added 0.4 equiv of FeCl<sub>3</sub>·6H<sub>2</sub>O (0.69 g) dissolved in distilled water (30 mL) dropwise over a 15-min interval. The deep purple solution was refluxed for an additional 40 min, cooled to room temperature, and finally vacuum-filtered to collect the uncomplexed ligand. After the free ligand was rinsed with ethanol until free of the purple complex, the filtrate was refiltered a second time and then rotary evaporated to dryness. A TLC of the resulting residue run on a silica gel 60 precoated plate with a mobile phase consisting of 7:3 chloroform/methanol gave a single spot with R<sub>f</sub> = 0.31. A reference sample obtained from 1:1 iron(III)/TMPHPG gave two spots of equal intensity with R<sub>f1</sub> = 0.38 and R<sub>f2</sub> = 0.31. The metal-free ligand was obtained as previously described.<sup>1</sup> The recovered amount was 0.93 g of *meso*-TMPHPG.

The racemic diastereomer was obtained by a second partial complexation of a sample of TMPHPG already enriched in the racemic pair through removal of a significant fraction of meso isomer by the procedure described above. Racemic isomer enriched TMPHPG (2.37 g, 5.3 mmol) was partially complexed with 0.4 equiv of iron(III). The uncomplexed ligand was collected and reprecipitated at pH 4–5 from a basic aqueous solution (pH 10) to remove trapped iron chelate. The recovered amount of *rac*-TMPHPG was 1.33 g. The purity of both diastereomers was confirmed by NMR spectra of the metal-free ligands, which show a pH-dependent shift of the proton on the chiral carbons (see Results).

**Preparation of Ga(III)-TMPHPG Complexes for NMR Spectroscopy.** Gallium(III) complexes of each diastereomer were prepared by first evaporating 40 mL of a GaCl<sub>3</sub> stock solution (9.12 × 10<sup>-3</sup> M) in 1.0-mL fractions with a 700 °C heat gun under N<sub>2</sub> flow. The resulting residue was redissolved in 1.0 mL of D<sub>2</sub>O, and the solution was again evaporated to dryness. TMPHPG (13.5 mg) was dissolved in a basic D<sub>2</sub>O solution, the solution combined with the GaCl<sub>3</sub> residue, and the pD adjusted to 9. The solution was heated briefly (10 min) at 80 °C and centrifuged and a final pD determined.

- (1) Bannochie, C. J.; Martell, A. E. *J. Am. Chem. Soc.* **1989**, *111*, 4735.
- (2) Madsen, S. L.; Bannochie, C. J.; Martell, A. E.; Mathias, E. J.; Welch, M. J. *J. Nucl. Med.*, in press.
- (3) Schwarzenbach, G.; Flaschka, M. *Complexometric Titrations*; Methuen: London, 1969.

<sup>†</sup> Present address: The Edward Mallinckrodt Institute of Radiology, Washington University School of Medicine, St. Louis, MO 63110.

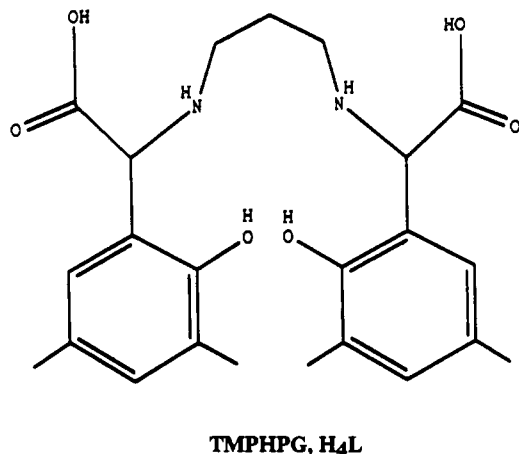


Figure 1.

**Potentiometric Equilibrium Determinations.** Equipment, calibration methods, and procedures are as previously described.<sup>1</sup> Throughout this paper  $-\log [H^+]$  is designated  $p[H]$ . Due to the tendency of each ligand to precipitate below  $p[H]$  5 at the concentrations used in the potentiometric measurements ( $2.00 \times 10^{-3}$  M ligand and metal), all data, unless otherwise noted, were obtained by back-titration with aqueous 0.1000 M HCl titrant after adjusting the experimental solution to between  $p[H]$  10 and 11.5 with standard aqueous 0.1000 M KOH. Fresh solutions of the ligand were prepared under  $N_2$  with 2 equiv of base prior to each experiment. The sluggish equilibration kinetics involving the gallium(III) systems resulted in precipitate formation from the experimental solutions at the above concentrations. In order to maintain a supersaturated solution through the insoluble region following the break in the back-titration, ligand and metal concentrations in the test solutions were made  $4.00 \times 10^{-4}$  M, and 0.020-mL additions of standard aqueous acid were made with a Gilmont screw-type microburet (0.002-mL graduations). With respect to indium(III), experimental solutions were prepared as described above but following initial mixing the solution was lowered to  $a \leq 0$  (where  $a$  is the ratio of the millimoles of base added to the millimoles of ligand present) and titrated with standard aqueous base.

The third through sixth ligand protonation constants as well as chelate protonation, stability, and hydrolysis constants for the 1:1 metal/ligand systems were calculated by the use of the FORTRAN program BEST.<sup>4</sup> The methods used in the computation have been described in detail elsewhere.<sup>5</sup>

**Spectrophotometric Equilibrium Measurements.** For the high- $p[H]$  spectra required to measure  $K_1^H$  and  $K_2^H$  for each of the TMPHPG ligands, 16–25 solutions were prepared with appropriate concentrations of 0.1000 M KOH to achieve incremental  $p[H]$  values. The  $pK_w$  used in the calculations of  $p[H]$  was  $-13.79$ . Each solution was brought to 10.00 mL by addition of 0.100 M KCl and had a final ligand concentration of  $1.40 \times 10^{-4}$  M. All test solutions were blanketed with argon and kept sealed prior to spectral measurements between 250 and 350 nm. Extinction coefficients and protonation constants for the phenolic protons were determined from the ultraviolet absorption band for the phenolate chromophore by using the FORTRAN program ABSPKAS written in this laboratory. Extinction coefficients and/or log protonation constants were adjusted to give the best agreement between the calculated and observed absorbance for each spectrum.

Stability constants for the iron(III) complexes were calculated from the visible absorption bands given in Table III for each system by using the BASIC program KML. Ligand protonation and chelate protonation constants were determined potentiometrically and spectrophotometrically in separate experiments. The extinction coefficients for the iron complex of each diastereomer were determined from the maximum observed absorbance and supplied to the program along with the absorbance, measured  $p[H]$ , and volume parameters for each system. The program calculates a log  $K_{ML}$  value for each absorbance and then recalculates the absorbance, percent free metal ion, and percent complex at each experimental point from the average log  $K_{ML}$ . In each case the extinction coefficient for the protonated metal chelate was unknown and was therefore varied to give the best agreement between observed and calculated absorbances. For the indium(III) *meso*-TMPHPG complex the chelate protonation constant was varied iteratively along with the un-

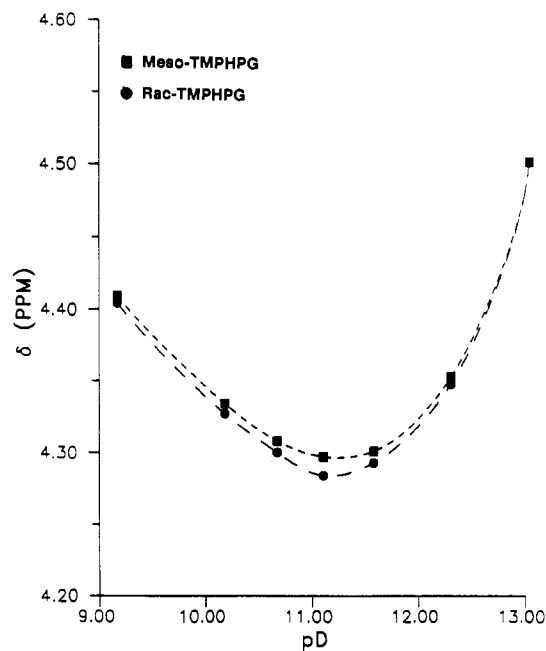


Figure 2. Effect of  $pD$  on the chemical shift ( $\delta$ ), relative to TSP, of the TMPHPG  $\alpha$ -chiral carbon proton resonance (400 MHz).

Table I. NMR Parameters (ppm) for Selected Resonances for Ga(III) Complexes of TMPHPG and EHPG in  $D_2O$  (300 MHz) Relative to TSP

ligand	$\alpha$ -H	$NCH_2CH_2N$	$NCH_2CH_2CH_2N$	$pD$
<i>rac</i> -TMPHPG	4.14 (s, 2 H)	3.46 (m, 2 H)	2.83 (m, 2 H)	8.74
			1.73 (m, 2 H)	
			3.24 (m, 1 H)	
<i>meso</i> -TMPHPG	4.33 (s, 1 H)	4.14 (s, 1 H)	3.09 (m, 1 H)	9.11
			2.88 (m, 1 H)	
			2.61 (m, 1 H)	
<i>rac</i> -EHPG	4.48 (s, 2 H)	3.41 (m, 2 H)	7.45	
		2.40 (m, 2 H)		
<i>meso</i> -EHPG	4.70 (s, 1 H)	4.51 (s, 1 H)	3.52 (m, 1 H)	8.35
			3.01 (m, 1 H)	
			2.44 (m, 2 H)	

known extinction  $\epsilon_{MHL}$ , in order to arrive at final best fit value of  $K_{ML}$ . Data taken in the range between where there was at least 10% free metal ion and 10% metal complex were used in the final calculation of log  $K_{ML}$ .

## Results

**Separation and Assignment of TMPHPG Diastereomers.** Two diastereomeric forms, a pair of enantiomers and a meso compound, arise in the synthesis of TMPHPG. Both diastereomers have been distinguished by  $^1H$  NMR spectra of the metal-free ligands. The hydrogen atoms on the chiral carbon centers show a pH-dependent shift, but unlike EHPG,<sup>6</sup> the two forms never differ by more than 0.015 ppm (Figure 2). As expected, the diastereotopic protons of the diamine alkyl chain also have different chemical shifts for the two forms. A similar situation occurs in EHPG, which has been incorrectly attributed to the diamine alkyl chain being "locked" in a particular conformation.<sup>7</sup>

By exploiting an expected difference in the stabilities of the iron(III) complexes of the two compounds, it was possible to isolate each diastereomer. In order to achieve partitioning of the 0.4 equiv of iron(III) to just one isomer, it was necessary to add 1.6 equiv of sodium bicarbonate. When an amount equivalent to the added iron (0.4 equiv) was used, the separation is poor as a result of formation of a neutral iron complex that precipitates from solution. The iron chelates of both diastereomers can be visualized by TLC using a silica gel 60 plate with a mobile phase of 7:3 chloroform/methanol. For  $Fe(rac\text{-}TMPHPG)$ ,  $R_f = 0.38$ , and for

(4) Motekaitis, R. J.; Martell, A. E. *Can. J. Chem.* **1982**, *60*, 2403.

(5) Martell, A. E.; Motekaitis, R. J. *Determination and Use of Stability Constants*; VCH Publishers: New York, 1989.

(6) Bonadies, J. A.; Carrano, C. J. *J. Am. Chem. Soc.* **1986**, *108*, 4088.

(7) Patch, M. G.; Simolo, K. P.; Carrano, C. J. *Inorg. Chem.* **1982**, *21*, 2972.

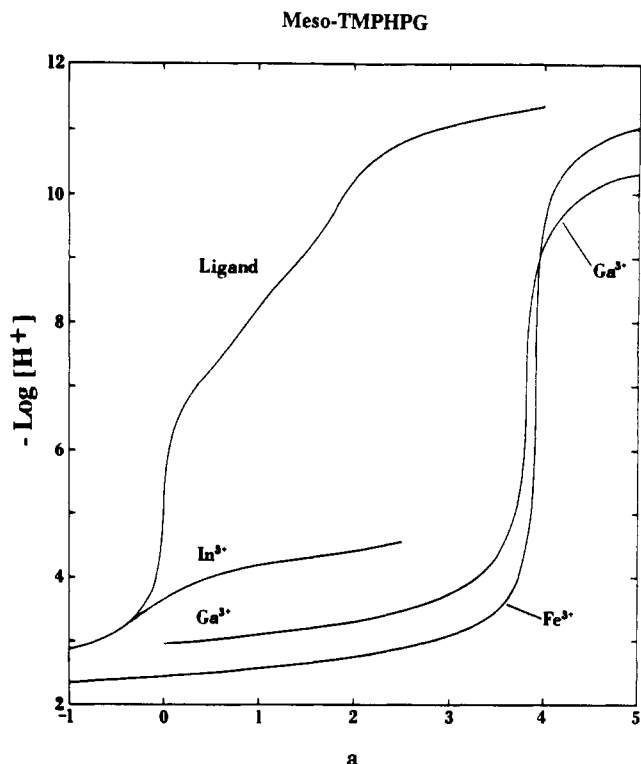


**Figure 3.** Potentiometric equilibrium curves for *meso*-TMPHPG systems. Initial concentrations: ligand alone  $1.94 \times 10^{-3}$  M;  $[\text{Fe}^{3+}]_{\text{tot}} = 1.86 \times 10^{-3}$  M and  $[\text{L}]_{\text{tot}} = 1.88 \times 10^{-3}$  M;  $[\text{Ga}^{3+}]_{\text{tot}} = 4.23 \times 10^{-4}$  M and  $[\text{L}]_{\text{tot}} = 4.32 \times 10^{-4}$  M;  $[\text{In}^{3+}]_{\text{tot}} = 1.02 \times 10^{-3}$  M and  $[\text{L}]_{\text{tot}} = 1.03 \times 10^{-3}$  M.  $t = 25.0$  °C;  $\mu = 0.10$  M (KCl);  $a$  is the moles of standard KOH solution added per mole of ligand present.

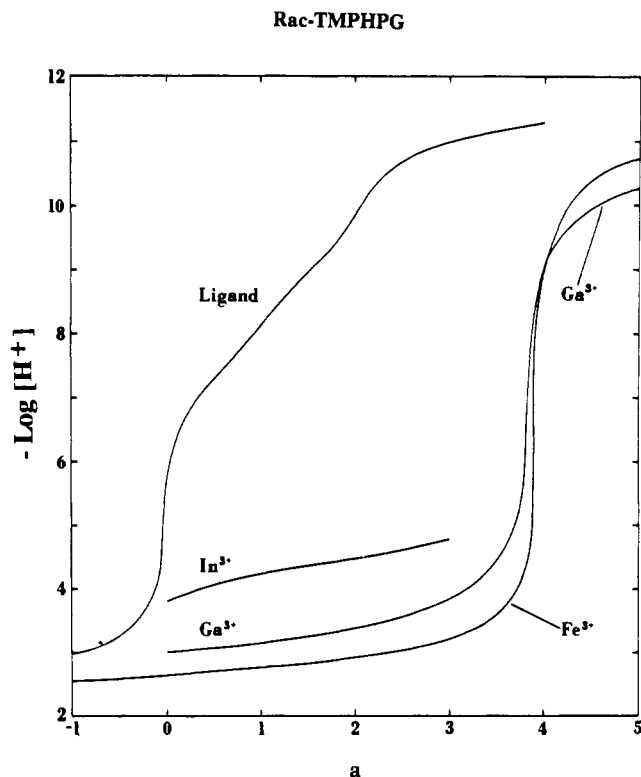


**Figure 4.** Potentiometric equilibrium curves for *rac*-TMPHPG systems. Initial concentrations: ligand alone  $1.92 \times 10^{-3}$  M;  $[\text{Fe}^{3+}]_{\text{tot}} = 9.73 \times 10^{-4}$  M and  $[\text{L}]_{\text{tot}} = 9.97 \times 10^{-4}$  M;  $[\text{Ga}^{3+}]_{\text{tot}} = 4.19 \times 10^{-4}$  M and  $[\text{L}]_{\text{tot}} = 4.28 \times 10^{-4}$  M;  $[\text{In}^{3+}]_{\text{tot}} = 9.91 \times 10^{-4}$  M and  $[\text{L}]_{\text{tot}} = 1.02 \times 10^{-3}$  M.  $t = 25.0$  °C;  $\mu = 0.10$  M (KCl);  $a$  is the moles of standard KOH solution added per mole of ligand present.

**Table II.** log Protonation Constants<sup>a</sup> for TMPHPG and EHPG<sup>b</sup>

constant	quotient	<i>rac</i> -TMPHPG	<i>meso</i> -TMPHPG	<i>rac</i> -EHPG	<i>meso</i> -EHPG
$K_1^{\text{H}}$	$[\text{HL}]/[\text{H}][\text{L}]$	12.56	12.98	12.05	11.90
$K_2^{\text{H}}$	$[\text{H}_2\text{L}]/[\text{H}][\text{HL}]$	11.65	12.08	10.87	10.85
$K_3^{\text{H}}$	$[\text{H}_3\text{L}]/[\text{H}][\text{H}_2\text{L}]$	8.94	9.14	8.79	8.76
$K_4^{\text{H}}$	$[\text{H}_4\text{L}]/[\text{H}][\text{H}_3\text{L}]$	7.33	7.33	6.33	6.36
$K_5^{\text{H}}$	$[\text{H}_5\text{L}]/[\text{H}][\text{H}_4\text{L}]$	2.49	2.29		
$K_6^{\text{H}}$	$[\text{H}_6\text{L}]/[\text{H}][\text{H}_5\text{L}]$	2.42	1.8		
$\sigma_{\text{H}}$		0.004	0.007	0.002	0.006

<sup>a</sup> $\mu = 0.10$  M (KCl);  $t = 25.0$  °C. <sup>b</sup>Reference 1.

$\text{Fe}(\text{meso-TMPHPG})$ ,  $R_f = 0.31$ . Dry column chromatography,<sup>8</sup> which proved to be very useful in the separation of *rac*- and *meso*-EHPG,<sup>1</sup> gave very poor resolution of the two bands due to the speed at which the column develops in this mobile phase.

In order to definitively assign each of the diastereomers, it was necessary to look at the <sup>1</sup>H NMR spectra of their respective gallium complexes. Table I provides a listing of the NMR parameters for the  $\alpha$ -H and diamine bridge proton signals for both the diastereomeric TMPHPG complexes as well as for those of EHPG. One will note that the  $\alpha$ -H signal is split into two singlets for each of the *meso* complexes, indicating that the hydrogen on each of the two chiral centers (which have opposite absolute configurations) has a different environment. On the other hand, the racemic complexes, which have the same absolute configurations at each of the two chiral centers (either R,R or S,S), have the two  $\alpha$ -H in equivalent chemical environments. Further dis-

**Table III.** Phenolate Absorption Bands and Extinction Coefficients of TMPHPG and EHPG<sup>a</sup>

ligand	$\lambda_{\text{max}}$	$\epsilon_{\text{L}}$	$\epsilon_{\text{HL}}$	$\epsilon_{\text{H}_2\text{L}}$
<i>rac</i> -TMPHPG	305	9020	4500	1820
<i>meso</i> -TMPHPG	304	8300	6480	2270
<i>rac</i> -EHPG	296	8610	6240	1980
<i>meso</i> -EHPG	296	8400	5730	1880

<sup>a</sup> $\mu = 0.10$  M (KCl);  $t = 25.0$  °C.

**Table IV.** TMPHPG Absorbance Changes with Ionic Strength

ligand	$\mu$	$\text{p}[\text{H}]_{\text{calc}}^a$	$A_{304}$	$A_{305}$	$A_{306}$
<i>rac</i> -TMPHPG	3.00	14.50		1.246	1.249
<i>rac</i> -TMPHPG	2.50	14.35		1.243	1.246
<i>meso</i> -TMPHPG	3.00	14.50	1.125	1.132	
<i>meso</i> -TMPHPG	2.50	14.35	1.123	1.130	

<sup>a</sup> $\text{p}K_w$  from a plot of  $\text{p}K_w$  vs  $\mu$  as determined by Harned and Owen (1958):  $\text{p}K_w = -14.02$ ,  $\mu = 3.00$ ;  $\text{p}K_w = -13.96$ ,  $\mu = 2.50$ .

cussion of the coordination geometries of these complexes will follow.

**Ligand Protonation Equilibrium Measurements.** Presented in Figures 3 and 4 are the potentiometric equilibrium curves for *meso*- and *rac*-TMPHPG, respectively, as well as their 1:1 metal/ligand  $\text{p}[\text{H}]$  profiles with  $\text{Fe}(\text{III})$ ,  $\text{Ga}(\text{III})$ , and  $\text{In}(\text{III})$ .

The first two protonations for each ligand,  $K_1^{\text{H}}$  and  $K_2^{\text{H}}$  (Table II), correspond to phenolate oxygen protonations and were determined spectrophotometrically from the phenolate ultraviolet absorption bands given in Table III, which also lists the extinction coefficients found in each of these ligands. Due to the high basicity of the phenolic oxygens in TMPHPG, it is not possible to determine the extinction coefficients for the fully deprotonated ligand at an ionic strength of 0.10. Therefore, in order to determine a value for these extinctions, absorbances were measured at ionic strengths of 2.5 and 3.0, as shown in Table IV. For each ligand the wavelength of maximum absorbance increases by 1 nm over

(8) Loev, B.; Goodman, M. N. *Progress in Separations and Purifications*; Interscience: New York, 1970; Vol. III, p 73.

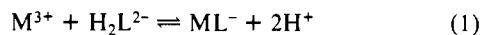
Table V. log Stability Constants<sup>a</sup> of Trivalent Metal Ions with TMPHPG and EHPG

metal ion	quotient	rac-TMPHPG <sup>b</sup>	meso-TMPHPG <sup>c</sup>	rac-EHPG <sup>d</sup>	meso-EHPG <sup>e</sup>
Fe <sup>3+</sup>	[ML]/[M][L]	34.22 ± 0.05	34.83 ± 0.03	35.54 ± 0.05	33.28 ± 0.04
	[MHL]/[H][ML]	2.71	2.98		2.72
	[ML]/[H][MOHL]	11.31	12.03	11.78	10.45
Ga <sup>3+</sup>	[ML]/[M][L]	32.46	33.96	33.89	32.40
	[MHL]/[H][ML]	3.91	3.70	2.22	3.44
In <sup>3+</sup>	[ML]/[M][L]	25.99	26.60 ± 0.05	26.68	25.26
	[MHL]/[H][ML]	4.26	5.20	4.47	6.14
	[MH <sub>2</sub> L]/[H][MHL]			4.78	3.42
	[ML]/[H][MOHL]			10.57	8.83

<sup>a</sup>  $\mu = 0.10$  M (KCl);  $t = 25.0$  °C. <sup>b</sup>  $\sigma_{\text{fit}}$ : Fe<sup>3+</sup>, 0.004; Ga<sup>3+</sup>, 0.010; In<sup>3+</sup>, 0.005.  $Q_{\text{fit}}$ : Fe<sup>3+</sup>, 0.40. <sup>c</sup>  $\sigma_{\text{fit}}$ : Fe<sup>3+</sup>, 0.003; Ga<sup>3+</sup>, 0.006.  $Q_{\text{fit}}$ : Fe<sup>3+</sup>, 0.14; In<sup>3+</sup>, 0.11. <sup>d</sup>  $\sigma_{\text{fit}}$ : Fe<sup>3+</sup>, 0.008; Ga<sup>3+</sup>, 0.003; In<sup>3+</sup>, 0.010.  $Q_{\text{fit}}$ : Fe<sup>3+</sup>, 0.30. <sup>e</sup>  $\sigma_{\text{fit}}$ : Fe<sup>3+</sup>, 0.005; Ga<sup>3+</sup>, 0.005; In<sup>3+</sup>, 0.004.  $Q_{\text{fit}}$ : Fe<sup>3+</sup>, 0.15.

that observed at  $\mu = 0.10$ , probably as a result of a small degree of association with the high concentration of potassium ions. The change in absorbance on going from  $\mu = 2.5$  to  $3.0$  is small and within experimental uncertainty; hence, the final extinctions for each ligand were determined from the data at  $\mu = 3.0$ . It is necessary to turn to spectrophotometry in the determination of protonation constants approaching 12 or more log units because they are beyond the limits of the potentiometric method. At this p[H], hydroxide ion becomes the predominant conveyor of charge rather than the supporting electrolyte, resulting in variations in junction potential. Additionally, small changes in p[H] as a result of buffering by solution species are washed-out by the high concentration of hydroxide ion and subject to considerable error.

An example of the spectroscopic equilibrium curves used in the determination of  $K_1^{\text{H}}$  and  $K_2^{\text{H}}$  is provided in Figure 5. A plot of absorbance versus p[H] for the TMPHPG ligands reveals an essentially straight line due to the overlapping nature of the first and second protonation constants. The FORTRAN program ABSPKAS varies the unknown extinction coefficients and log protonation constants to achieve the best possible fit between the observed and calculated absorbances. Even when  $\epsilon_{\text{L}}$  is determined separately and fixed, as was done in these experiments, four parameters remain,  $\epsilon_{\text{HL}}$ ,  $\epsilon_{\text{H}_2\text{L}}$ ,  $K_1^{\text{H}}$ , and  $K_2^{\text{H}}$ , and they are used to fit the absorbance versus p[H] data. Since a straight line can be defined with only two parameters, there are uncertainties with regard to the uniqueness of a particular set of values. It is difficult to predict the values of the unknown extinctions because of the presence of microspecies. For instance, intuitively the value of  $\epsilon_{\text{H}_2\text{L}}$  should be nearly zero, since the fully protonated phenols have essentially no absorbance at the wavelength corresponding to their deprotonation, but as a result of microspecies, one continues to see a change in the absorbance at the phenolate band until below p[H] 3, well below the protonation constants of the two phenolate oxygens. The constants listed in Table II represent macroscopic protonation constants but the determination of protonation constants from spectroscopic data is influenced by the presence of microspecies and their effect on the extinction coefficients. Providing sufficient spectroscopic data is important to minimize the number of solutions from a statistical perspective, but experimental limitations remain when protonation constants are overlapping. With this in mind, the values of  $\log K_1^{\text{H}}$  and  $K_2^{\text{H}}$  for rac- and meso-TMPHPG are considered the best possible estimates of these constants. In order that any error in these values not influence the interpretation of the metal binding affinities, they can be subtracted from the calculated chelate stability constants, leaving these to be compared as dissociation constants as expressed below in eqs 1 and 2. A discussion of the limitations of this procedure and its significance to the interpretation of the data is left until a later section.



$$K = \frac{[\text{ML}][\text{H}]^2}{[\text{M}][\text{H}_2\text{L}]} \quad (2)$$

Log  $K_3^{\text{H}}$ ,  $K_4^{\text{H}}$ ,  $K_5^{\text{H}}$ , and  $K_6^{\text{H}}$  (Table II) were determined by potentiometric back-titration. These data were analyzed with the FORTRAN program BEST<sup>4</sup> written in this laboratory. Protonation constants were varied to achieve the best possible fit between the

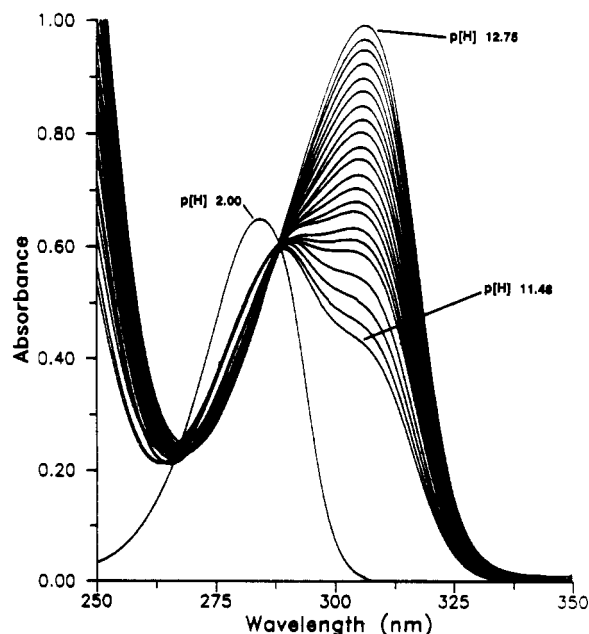
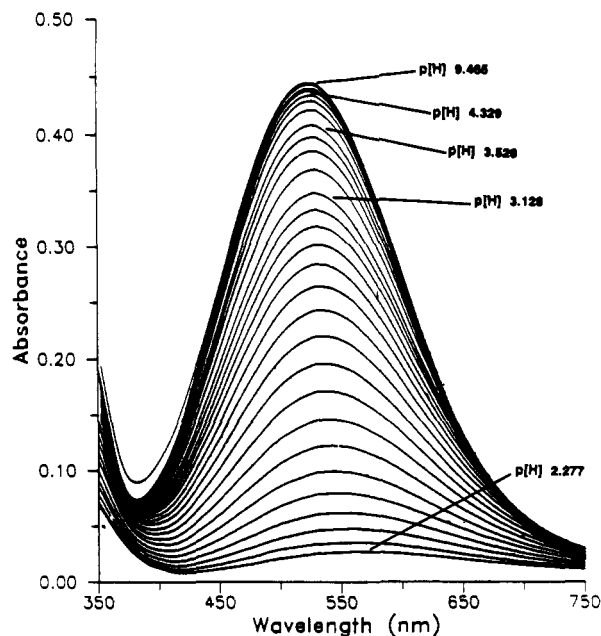


Figure 5. UV absorption spectra of rac-TMPHPG as a function of p[H]. [*rac*-TMPHPG] =  $1.38 \times 10^{-4}$  M;  $t = 25.0$  °C;  $\mu = 0.100$  M (KCl + KOH). p[H] increment is 0.10 from p[H] 11.48 to 11.90 and 0.05 from p[H] 11.90 to 12.75.

observed and calculated p[H] at each datum point according to the stoichiometric parameters supplied.  $K_3^{\text{H}}$  and  $K_4^{\text{H}}$  correspond to the protonation constants of the secondary amine nitrogens, and  $K_5^{\text{H}}$  and  $K_6^{\text{H}}$ , to protonation of the carboxylate oxygens. It should be noted that *rac*-TMPHPG will readily precipitate on standing at 4 equiv of acid but it is possible to titrate a supersaturated solution of this ligand quickly beyond this point.

**Metal Ion Affinity Measurements.** The affinities of both diastereomers of TMPHPG for the radiopharmaceutically relevant metal ions iron(III), gallium(III), and indium(III) were measured. The methods used to overcome a number of solubility problems encountered are addressed in the Discussion, which follows the results for each metal ion system. Table V provides the calculated results of the equilibrium work done with each diastereomer and should be referred to as necessary.

The potentiometric equilibrium data in Figures 3 and 4 indicate that both forms of TMPHPG lose essentially four protons upon complexation with iron(III), as well as with gallium(III). However, displacement is not complete as was true for [Fe(*meso*-EHPG)], and a protonated metal chelate equilibrium constant can be calculated from these data. The presence of a protonated species is also evident in the spectroscopic equilibrium curves for the two iron(III) systems. It is shown in Figure 6 for Fe(*rac*-TMPHPG) by the gradual shift to higher wavelengths as the p[H] decreases. The presence of hydroxo metal chelates for both ligands was also evident in the potentiometric data by the buffering observed in the curve beyond an  $a$  value of 4. The presence of this species seems to indicate that there is still sufficient strain in these metal complexes to facilitate replacement of one of the carboxylate



**Figure 6.** Effect of  $p[H]$  on the optical spectrum of  $Fe(rac\text{-}TMPHPG)$ . Initial concentrations:  $[Fe^{3+}] = 9.88 \times 10^{-5} M$ ;  $[rac\text{-}TMPHPG] = 9.93 \times 10^{-5} M$ . Spectra are shown uncorrected for dilution;  $t = 25.0^\circ C$ ;  $\mu = 0.10 M$  (KCl).  $p[H]$  increment is 0.05 from  $p[H]$  2.277 to 3.128, 0.10 from  $p[H]$  3.128 to 3.526, and 0.20 from  $p[H]$  3.526 to 4.329.

**Table VI.** Visible Absorption Bands and Extinction Coefficients of Iron(III) Complexes of TMPHPG and EHPG<sup>a</sup>

ligand	$\lambda_{max}$	$\epsilon_{ML}$	$\epsilon_{MHL}$
<i>rac</i> -TMPHPG	535	5140	2140
<i>meso</i> -TMPHPG	530	4470	2980
<i>rac</i> -EHPG	480	4850	
<i>meso</i> -EHPG	485	4280	2740

<sup>a</sup>  $\mu = 0.10 M$  (KCl);  $t = 25.0^\circ C$ .

oxygens by a hydroxide ion. One will note that (EHPG)iron(III) complexes, which also have hydroxo chelates, are six-coordinate rather than seven-coordinate as in iron(III) EDTA.<sup>9,10</sup> Since water is excluded from the inner coordination sphere, loss of a proton from a coordinated water molecule is not possible.

While there is sufficient free metal ion in the potentiometric equilibrium measurements ( $\approx 10\%$ ) to determine the formation constants for each diastereomer, the solubility product of  $Fe(OH)_3$  has been exceeded. Due to the intense purple color of these complexes it is not possible to determine whether small amounts of precipitate are present or not. Hence, these formation constants were determined spectroscopically. The spectral characteristics used to determine the formation constants for each TMPHPG diastereomer are presented in Table VI along with those for EHPG. The absorbance maxima for the two complexes of TMPHPG differ by 5 nm, as was the difference between *rac*- and *meso*-EHPG. The value of  $\epsilon_{MHL}$  (Table VI) found in each case indicates that the site of protonation in the metal chelates probably corresponds to one of the phenols, since the extinction coefficient is roughly half that of the final complex, which presumably involves both phenolate oxygens.

During examination of the gallium(III) systems it was observed that in the potentiometric back-titration that followed the observed break in the curve at an  $a$  value of 4 the slower equilibrating gallium(III) systems permitted precipitate formation at the usual component concentrations employed in potentiometric work ( $2.00 \times 10^{-3}$  or  $1.00 \times 10^{-3} M$ ). The curves presented in Figures 3 and 4 were obtained by lowering the metal and ligand concentrations

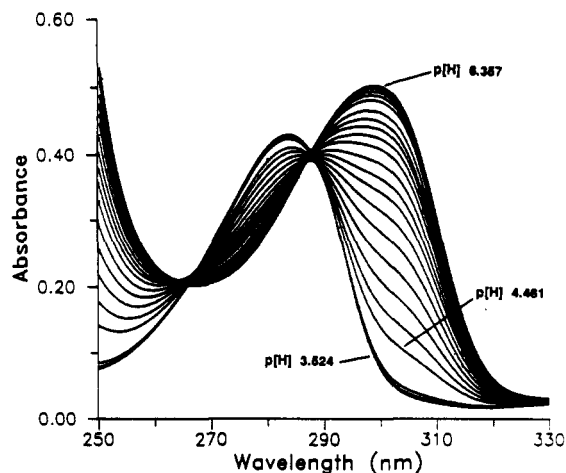


**Figure 7.** Effect of  $p[H]$  on the ultraviolet spectrum of  $In(meso\text{-}TMPHPG)$ . Initial concentrations:  $[In^{3+}] = 9.81 \times 10^{-5} M$ ;  $[meso\text{-}TMPHPG] = 9.90 \times 10^{-5} M$ . Spectra are shown uncorrected for dilution;  $t = 25.0^\circ C$ ;  $\mu = 0.10 M$  (KCl).  $p[H]$  increment is 0.10 from  $p[H]$  4.461 to 6.357.

to  $4.00 \times 10^{-4} M$ , or one-fifth the usual value, thus permitting titration of a supersaturated solution through this slowly equilibrating region of the curve. The introduction of standard acid to the solution through the use of the Gilmont microburet, with its 0.002-mL graduation, permitted reasonably accurate additions of the small volumes required. It should be cautioned that because of the dilute conditions there is a tendency for error to be magnified in these measurements. The  $\sigma_{fit}$  given in Table V for these systems is quite good given the high dilution. Sufficient free gallium at an  $a$  value of zero ( $\approx 18\%$ ) permitted calculation of the formation constants for these systems. Unlike either form of EHPG the equilibria beyond an  $a$  value of 4 are between the metal ion complex and gallate, indicating that the complex cannot resist beyond  $p[H]$  10 the high stability and strong tendency that gallium(III) has toward formation of this tetrahydroxometal species and hence no hydroxometal chelate exists at measurable levels.

In the determination of the formation constants for *rac*- and *meso*-TMPHPG with indium(III), a significantly reduced affinity was evident. There was a tendency for precipitate formation at  $p[H]$  4.5 for both ligands, which is due to  $In(OH)_3$  and/or a neutral metal complex. Formation of the complex at a higher  $p[H]$  also resulted in a precipitate. In the case of *rac*-TMPHPG the partial curve from  $a = 0-3$  (Figure 4) was employed in the determination of the formation constant of the complex. Replicate experiments gave nearly identical values. In the case of the other diastereomer, *meso*-TMPHPG, a precipitate formed repeatedly prior to an  $a$  value of three. Rather than use this extremely fragmentary data to access the formation constant, the value shown in Table V was determined spectrophotometrically from the equilibrium curves shown in Figure 7. The absorption band at 298 nm results from phenolate oxygen involvement in the metal complex and represents a 6-nm shift from the band that occurs at high  $p[H]$  for the ligand alone (Table III). Essentially no change occurs at 298 nm between  $p[H]$  3.0 and 6.6 in the absence of indium(III). An extinction coefficient for  $\epsilon_{ML}$  of 5580 was determined at  $p[H]$  9.7. The later changes in the absorbance evident in Figure 7 correspond essentially, but not entirely, to deprotonation of a protonated metal chelate. Due to dilute,  $1.0 \times 10^{-4} M$ , concentrations employed in spectrophotometric measurements, one is able to follow this formation well beyond the  $p[H]$  where initial free indium hydrolysis occurs ( $p[H]$  4.31).<sup>11</sup> A value of  $K_{ML}$  was found by iterating the values of the unknown  $\epsilon_{MHL}$  and  $K_{ML}^H$  (chelate protonation constant) to give the best agreement between the observed and calculated absorbances.

(9) Roe, A. L.; Schneider, D. J.; Mayer, R. J.; Pyrz, J. W.; Widon, J.; Que, L., Jr. *J. Am. Chem. Soc.* **1984**, *106*, 1676.  
 (10) Graf, E.; Mahoney, J. R.; Bryant, R. G.; Eaton, J. W. *J. Biol. Chem.* **1984**, *259*, 3620.

(11) Brown, P. L.; Ellis, J.; Sylva, R. N. *J. Chem. Soc., Dalton Trans.* **1982**, 1911.

**Table VII.** log Protonation and Stability Constants of Other Diastereomeric Ligands<sup>a</sup>

quotient	<i>d</i> -TA <sup>b</sup>	<i>meso</i> -TA <sup>b</sup>	<i>rac</i> -DBTA <sup>c</sup>	<i>meso</i> -DBTA <sup>c</sup>	<i>rac</i> -DBTA-DA <sup>d</sup>	<i>meso</i> -DBTA-DA <sup>d</sup>
[HL]/[H][L]	3.97	4.49	11.61	11.23	8.41	6.87
[H <sub>2</sub> L]/[H][HL]	2.82	2.97	6.09	6.28	3.90	3.63
[H <sub>3</sub> L]/[H][H <sub>2</sub> L]			3.49	2.6	1.8	1.5
[H <sub>4</sub> L]/[H][H <sub>3</sub> L]			2.40	1.8		
[NiL]/[Ni][L]			22.4	20.2		
[CuL]/[Cu][L]	2.65 <sup>e</sup>	3.15 <sup>e</sup>	21.6	19.8	12.63	11.72
[CuL <sub>2</sub> ]/[Cu][L] <sup>2</sup>	4.38 <sup>e</sup>	5.31 <sup>e</sup>				
[CuHL]/[H][CuL]			2.40	3.70		
[CuL]/[H][Cu(H <sub>-1</sub> L)]					7.93	8.15
[ZnL]/[Zn][L]			19.0	17.2	11.72	9.90
[ZnHL]/[H][ZnL]			2.57	3.52		1.45
[FeL]/[Fe <sup>3+</sup> ][L]		6.66	28.22	25.42		
[FeL <sub>2</sub> ]/[Fe <sup>3+</sup> ][L] <sup>2</sup>		12.30				
[InL]/[In][L]	4.44	4.97				
[InL <sub>2</sub> ]/[In][L] <sup>2</sup>	8.46 <sup>f</sup>	9.74				

<sup>a</sup> From ref 13. <sup>b</sup>  $\mu = 0.10$  M;  $t = 25.0$  °C. <sup>c</sup>  $\mu = 0.10$  M;  $20.0$  °C. <sup>d</sup>  $\mu = 0.15$  M;  $37.0$  °C. <sup>e</sup>  $\mu = 1.0$  M;  $t = 25.0$  °C. <sup>f</sup> Racemic mixture used.

Unlike *rac*- and *meso*-EHPG<sup>1</sup> no indication of a diprotonated metal complex was found for either TMPHPG diastereomer.

### Discussion

**TMPHPG Synthesis.** The low yield of TMPHPG, consistently <6%, was initially surprising but may be related to the basicity of the starting diamine. This Mannich-type reaction is believed to proceed, in most cases, by reaction of the free amine, rather than its hydrochloride, with the aldehyde followed by conversion to an iminium ion, thus requiring a small amount of acid, prior to reaction with an active substrate.<sup>12</sup> Hence, if the pH is too low the first step will not proceed. Likewise, if the pH is too high, there will be insufficient acid for the formation of iminium ion. Additionally, as the pH is raised, ever increasing quantities of the deprotonated phenol are produced.

**Proton Equilibria in Diastereomeric Ligands.** While published work with diastereomeric pairs of ligands is extremely limited, a survey<sup>13</sup> of ligand pairs that have been examined under the same conditions reveals that a variation in ligand protonation constants between diastereomers is the norm rather than the exception. Protonation constants and stability constants for the three pairs of ligands previously examined are provided in Table VII. The ligands consist of the well-known tartaric acid (TA) as well as two derivatives of EDTA, (1,2-dimethylethylene)dinitrilotetraacetic acid (DBTA) and (1,2-dimethylethylene)dinitrilodiacetamidodiacetic acid (DBTA-DA). Alkylation of the ethylene bridge in EDTA type ligands such as DBTA creates distinct sterically induced differences between the diastereomers, which result in the racemic ligands preferring a skew configuration over the trans configuration found in the *meso* ligands.<sup>14</sup> This distinction explains the variation observed in the protonation constants of Table VII in terms of hydrogen bonding and charge repulsions. In the case of EHPG and TMPHPG the situation is not as straight forward because, as stated previously, EHPG shows little or no diastereomeric differences whereas TMPHPG does. The difference apparently arises as a result of the additional methylene linkage, which gives rise to different hydrogen bonding and charge repulsions that affect the protonation constants. Unfortunately, an examination of molecular models gives no clear indication of these interactions.

**TMPHPG Metal Ion Affinities.** The relative weakness observed for the indium(III) complexes of TMPHPG as compared to their iron(III) and gallium(III) counterparts preserves a trend that has become apparent from this work and other recent work done in this research group. While a survey of indium(III) formation constants<sup>13</sup> will reveal that polyamino polycarboxylic acid donor ligands have roughly equivalent affinity for gallium(III) and

**Table VIII.** log Dissociation Constants<sup>a,b</sup> for Trivalent Metal Ions with TMPHPG and EHPG

metal ion	<i>rac</i> -TMPHPG	<i>meso</i> -TMPHPG	<i>rac</i> -EHPG	<i>meso</i> -EHPG
Fe <sup>3+</sup>	10.01	9.77	12.62	10.53
Ga <sup>3+</sup>	8.25	8.90	10.97	9.65
In <sup>3+</sup>	1.78	1.54	3.76	2.51

<sup>a</sup>  $\mu = 0.10$  M (KCl);  $t = 25.0$  °C. <sup>b</sup>  $K = [ML][H]^2/[M][H_2L]$ .

indium(III), the much harder phenol-containing donor ligands found in this and other work<sup>15,16</sup> indicate considerably reduced affinity for the softer indium(III) ion. These observations would dictate that indium(III) be considered independently from these other metal ions in the design of thermodynamically stable ligands.

If the stability constants for both diastereomers of TMPHPG are expressed as dissociation constants (eq 2) by subtracting out the contribution of the phenolate oxygen donor groups to the complex stability constant, some unexpected changes in the affinity trends are observed (Table VIII). Rather than *meso*-TMPHPG consistently having the higher affinities, there is a reversal for iron(III) and indium(III). The new affinity pattern follows the trend noted for the EHPG complexes, namely that the weaker complexes show the higher chelate protonation constants. It is also quite clear from the dissociation constants that the differences in stability between the pair of TMPHPG diastereomers is less than in those of EHPG for each of the metal ions.

However, two observations are not readily explained. The first is why iron(III) and gallium(III) show different preferences for the two diastereomers. The lower gallium(III) affinities relative to those of iron(III) can be attributed to the greater covalent character of the iron(III) coordinate bonds, but this does not explain the preference difference. The second unusual feature is why the greatest difference between the diastereomeric complexes is found between the two gallium(III) complexes. Biodistributions of these metal complexes in mature Sprague-Dawley rats also found the greatest difference in the liver uptake to be between the gallium(III) complexes.<sup>17</sup>

**Comparison of TMPHPG and EHPG.** Several factors contribute to differences in proton affinities between the two ligand pairs. As a result of the longer, more flexible trimethylene bridge in TMPHPG, the two secondary nitrogens are more independent of one another and hence more basic. The third protonation is facilitated by the ability of TMPHPG to form a six-membered hydrogen-bonded ring encompassing both amino nitrogens rather than the five-membered ring possible in EHPG. The preference of small metal ions for six-membered rings<sup>18</sup> is probably extendible

- (12) March J. *Advanced Organic Chemistry*; John Wiley & Sons: New York, 1985.  
 (13) Smith, R. M.; Martell, A. E. *Critical Stability Constants*; Plenum: New York, 1974, 1975, 1976, 1977, 1982, 1989; Vols. 1-6.  
 (14) Okaku, N.; Toyoda, K.; Moriguchi, Y.; Ueno, K. *Bull. Chem. Soc. Jpn.* **1967**, *40*, 2326.

- (15) Motekaitis, R. J.; Sun, Y.; Martell, A. E. *Inorg. Chim. Acta* **1989**, *159*, 29.  
 (16) Motekaitis, R. J.; Martell, A. E.; Welch, M. J. *Inorg. Chem.* **1990**, *29*, 1463.  
 (17) Madsen, S. L.; Bannochie, C. J.; Welch, M. J.; Mathias, C. J.; Martell, A. E. *Nucl. Med. Biol.* **1990**, *31*, 1662.  
 (18) Hancock, R. D.; Martell, A. E. *Comments Inorg. Chem.* **1988**, *6*, 237.

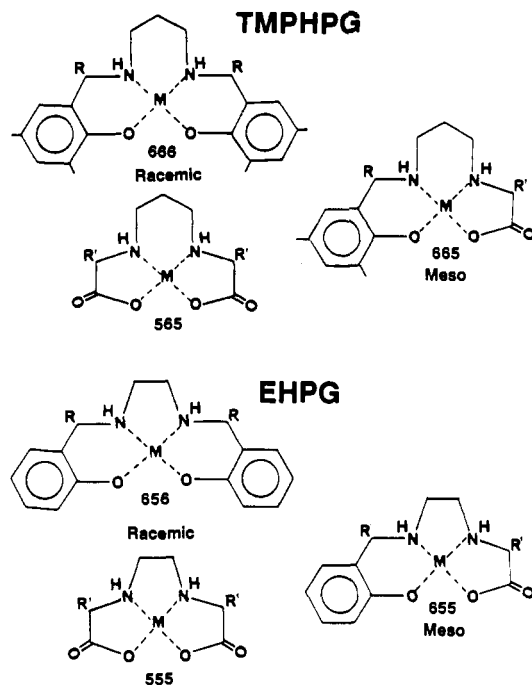


**Figure 8.** Possible ring conformations of EHPG and TMPHPG for the plane defined by the diamine ring in a hexacoordinate octahedral complex. R = -COOH and R' = *o*-hydroxyphenyl (EHPG) or 2-hydroxy-3,5-dimethylphenyl (TMPHPG).

into the regime of hydrogen bonding. Addition of a fourth equivalent of acid results in less charge repulsion between the nitrogens of TMPHPG and the value of  $\log K_4^H$  increases by 1 order of magnitude over that observed in EHPG (Table II). Methylation of the phenolic rings in the ortho and para positions increases the basicity of the phenolate oxygens as a result of inductive electron donation.

An essential difference between the two diastereomeric pairs of ligands that must be addressed in a comparison of their relative metal ion affinities is the alkyl chain length connecting the two hydroxyphenylglycine moieties. A summary of the chelate ring configurations of EHPG and TMPHPG for the plane defined by the diamine chelate ring is shown in Figure 8. In the numbering scheme employed, 5 or 6 refers to the number of members in each of the three chelate rings defining the plane, with the central digit always referring to the diamine chelate ring. It should be noted that these configurations of the chelate rings are only fixed when the ligands are fully coordinated to a metal ion; hence, they may not apply for the protonated metal chelates formed by most of these ligands. Only the 656 pattern has been found in the solid state for complexes of *rac*-EHPG.<sup>19,20</sup> Greater stability was proposed<sup>21</sup> and has been found<sup>1</sup> for the racemic ligand on the basis of more favorable octahedral geometry achieved by placement of both six-membered chelate rings with their greater bite in the plane defined by the ethylenediamine ring. Going from EHPG to TMPHPG changes the central chelate ring size from five to six. *rac*-TMPHPG also has two possible configurations of its chelate rings: 666 or 565. An examination of CPK molecular models indicates that when *rac*-TMPHPG is in the 666 configuration, the two carboxylate oxygens cannot quite reach the axial positions to satisfy an octahedral coordination environment. Hence, this particular configuration has considerable strain, while the 565 form is able to achieve a quite satisfactory octahedral environment. The 555 configuration is not found for *rac*-EHPG, but the corresponding 565 form for *rac*-TMPHPG is probably the preferred configuration.

**Table IX.**  $pM^a$  and  $\log K_{ML}$  Values for Trivalent Metal Ion Chelates

ligand	Fe(III)		Ga(III)		In(III)	
	$\log K_{ML}$	$pM$	$\log K_{ML}$	$pM$	$\log K_{ML}$	$pM$
<i>rac</i> -TMPHPG	34.22	22.0	32.46	20.2	25.99	13.8
<i>meso</i> -TMPHPG	34.83	21.6	33.96	20.7	26.60	13.3
<i>rac</i> -EHPG	35.54	25.0	33.89	23.3	26.68	16.1
<i>meso</i> -EHPG	33.28	22.9	32.40	22.0	25.26	14.9
HBED	39.68 <sup>b</sup>	28.8	39.57 <sup>c</sup>	28.7	30.9 <sup>d</sup>	20.0
PLED <sup>e</sup>	30.78	23.2	32.31	24.7	26.54	19.0
SHBED <sup>e</sup>	36.87	26.7	37.4	27.2	29.37	19.2
TMHBED <sup>f</sup>	37.41	24.4	34.19	21.2	30.72	17.8
TBHBED <sup>f</sup>	38.52	25.6	36.30	23.3	31.26	18.3
HBMA <sup>f</sup>	31.71	19.8	30.50	19.1	26.30	14.9
transferrin <sup>g</sup>	20.67 ( $K_2$ ) <sup>h</sup>		20.3 ( $K_1$ ) <sup>i</sup>		18.2 ( $K_1$ ) <sup>d</sup>	
	19.38 ( $K_2$ ) <sup>h</sup>	19.7	19.3 ( $K_2$ ) <sup>i</sup>	19.3	17.4 ( $K_2$ ) <sup>d</sup>	17.2

<sup>a</sup> Calculated for  $[L]_i = 1.1 \times 10^{-6}$  M,  $[M]_i = 1.0 \times 10^{-6}$  M, and  $p[H] = 7.40$ . <sup>b</sup> Reference 27. <sup>c</sup> Reference 28. <sup>d</sup> Estimated value. <sup>e</sup> Reference 15. <sup>f</sup> Reference 16. <sup>g</sup>  $K_1 = [MT_r]/[M][TR]$ ,  $K_2 = [M_2T_r]/[M][MTR]$ . <sup>h</sup>  $[HCO_3^-] = 1.4 \times 10^{-4}$  M. <sup>i</sup>  $[HCO_3^-] = 5.0 \times 10^{-3}$  M.<sup>30</sup>

Recently, Hancock and co-workers<sup>22-24</sup> have pointed out through the use of molecular mechanics calculations that the size of a metal ion is related to its preference for five- or six-membered chelate rings, with larger metal ion complexes being more destabilized by an increase in chelate ring size than the corresponding complexes of smaller metal ions. This observation satisfactorily explains the EDTA analogue TMDTA's weaker complexes with larger metal ions such as cadmium(II) and lanthanum(II) but more stable copper(II) complex when compared with the corresponding EDTA chelates.<sup>18</sup> TMDTA contains a trimethylenediamine bridge relative to the ethylene bridge in EDTA. Traditionally, the prevailing wisdom has been that five-membered chelate rings form more stable complexes than their six-membered counterparts, unless the six-membered chelate ring contains a double bond.<sup>25</sup> It is also commonly stated that six-membered chelate rings have a greater bite angle ( $90^\circ$ ) than those of five-membered chelate rings ( $70-80^\circ$ ) and thus can better fulfill an octahedral coordination environment.<sup>26</sup> The generality of any of these rules must be considered in light of the ability of a given ligand or configuration to satisfy the geometric requirements of a particular metal ion, especially when considering complexes of metal ions such as iron(III) and gallium(III), which are neither particularly large nor small. But a preference by larger metal ions for five-membered chelate rings, coupled with the high phenolate oxygen basicities, could explain the particularly poor affinity of both TMPHPG diastereomers for indium(III). At low  $p[H]$ , when protons complete successfully for the phenolate oxygens, neither TMPHPG ligand combines with indium(III) to form a diprotonated metal chelate as observed for *rac*- or *meso*-EHPG. A chelate ring size preference must also play a role in offsetting the higher affinity expected from iron(III) and gallium(III) for the two TMPHPG ligands over their EHPG counterparts as a result of the harder donor character of their substituted phenols. For iron(III) the greater stability imparted on the complexes at high  $p[H]$  by the substituted phenols is reflected by the higher value of the constants for hydroxo chelate formation in both *rac*- and *meso*-TMPHPG.

**Significance for Radiopharmaceuticals.** The existence of two diastereomeric forms of TMPHPG raises the possibility of different in vivo behavior for each metal complex especially in light of the significant variation in solution equilibria. A comparison of the total metal ion sequestering ability of a series of ligands can be made through calculation of  $pM$  values, where  $pM = -\log [M_f]$ . The calculation of  $[M_f]$ , the concentration of free aquo

(19) Bailey, N. A.; Cummins, D.; McKenzie, E. D.; Worthington, J. M. *Inorg. Chim. Acta* **1981**, *50*, 111.

(20) Riley, P. E.; Pecoraro, V. L.; Carrano, C. J.; Raymond, K. N. *Inorg. Chem.* **1983**, *22*, 3096.

(21) Bernauer, K. *Top. Curr. Chem.* **1976**, *65*, 1.

(22) Thom, V. J.; Hosken, G. D.; Hancock, R. D. *Inorg. Chem.* **1985**, *24*, 3378.

(23) Hancock, R. D. *Pure Appl. Chem.* **1986**, *58*, 1445.

(24) Hancock, R. D.; Martell, A. E. *Chem. Rev.* **1989**, *89*, 1875.

(25) Basolo, F.; Johnson, R. *Coordination Chemistry*; W. A. Benjamin, Inc.: New York, 1964.

(26) Pecoraro, V. L. Ph.D. Dissertation, University of California, Berkeley, CA, 1981.

metal ion, through the use of eq 3 takes into consideration the

$$[M_f] = \frac{\alpha_L T_M}{\alpha_{ML} K_{ML} (T_L - T_M)} \quad (3)$$

$$\alpha_L = 1 + \beta_n^H [H^+]^n \quad (4)$$

$$\alpha_{ML} = 1 + \beta_{MH_nL}^H [H^+]^n \quad (5)$$

proton affinities of the ligand,  $\alpha_L$  term, and other chelate species such as protonated metal complexes,  $\alpha_{ML}$  term. For metal complexes where the predominate chelate species is ML across the p[H] range of interest, the  $\alpha_{ML}$  term approaches unity and can be neglected in the calculation. The relative order of pM values given in Table IX holds only for the specified set of conditions, which include the metal ion concentration, ligand concentration, and p[H]. A higher ligand metal ion affinity is reflected by a greater pM value.

Table IX provides the value of pM calculated for each of the TMPHPG and EHPG ligands by employing a 10% excess of ligand at a physiologic p[H] of 7.4. Also provided are pM values for a variety of related multidentate ligands that have recently been investigated in this research group.<sup>16,18</sup> Since the stability constants of indium(III)-transferrin have not been accurately measured, the correlation between log  $K_{ML}$  values for the ligands of Table IX with iron(III) and indium(III) was employed to arrive at a reasonable estimate of log  $K_1^*$  and log  $K_2^*$  for indium(III)-transferrin.<sup>1</sup> The values of log  $K_1^*$  and by  $K_2^*$  estimated for indium(III)-transferrin are 18.2 and 17.4, respectively, at 25.0 °C,  $\mu = 0.10$  M, and  $[HCO_3^-] = 1.4 \times 10^{-4}$  M. It is clear that the iron(III) and gallium(III) TMPHPG complexes would be

expected to resist exchange of metal ion with transferrin in vivo. On the other hand, such an exchange is thermodynamically favorable for each of the indium(III) complexes.

### Conclusions

Selective complexation of one isomer with a metal ion can be a useful method for the separation of diastereomeric ligand pairs. The metal ion must form a stable complex involving all the ligand donor groups and have distinct coordination preferences that may be less favorable in one diastereomer than in the other.

The more lipophilic EHPG analogues, *rac*- and *meso*-TMPHPG, with their dimethylated phenyl rings and a longer diamine bridge maintain a very high affinity for iron(III) and gallium(III) but form even weaker complexes with indium(III) than was found for *rac*- and *meso*-EHPG. The increased separation of the two chiral centers in the TMPHPG diastereomers, by an additional methylene group, generally reduced the differences in stability observed between the diastereomeric complexes. A further increase in the diamine alkyl chain length will undoubtedly serve to further isolate the two phenylglycine moieties and result in an additional decrease in the difference in metal ion affinity displayed by the diastereomers.

The most notable feature of these ligands is their relatively poor affinity for indium(III). Clearly the results of this work, and additional recent work conducted in this research group,<sup>15,16</sup> have demonstrated the lower relative affinity of indium(III) for hard phenolate oxygen donor atoms as compared to iron(III) and gallium(III). Ligands with a high affinity for indium(III) should be designed separately from those found useful for iron(III) and gallium(III). The design of these ligands needs to take into consideration the larger size of indium(III) as well as incorporation of softer coordinate donor groups.

**Acknowledgment.** This research was supported by the U.S. Public Health Service, National Cancer Institute, Grant No. CA-42925, and The Robert A. Welch Foundation, Grant No. A-259.

(27) L'Éplattenier, F.; Murase, I.; Martell, A. E. *J. Am. Chem. Soc.* **1967**, *89*, 837.

(28) Harris, W. E.; Martell, A. E. *Inorg. Chem.* **1976**, *15*, 713.

(29) Aisen, P.; Liebman, A.; Zweier, J. *J. Biol. Chem.* **1978**, *253*, 1930.

(30) Harris, W. R.; Pecoraro, V. L. *Biochemistry* **1983**, *22*, 292.

Contribution from the Department of Chemistry, The University of Calgary, Calgary, Alberta, Canada T2N 1N4, and Department of Chemistry and Biochemistry, University of Arkansas, Fayetteville, Arkansas 72701

## Synthesis and Structure of the Norbornene Adduct of 1,3,5,2,4,6-Trithiatriazinium Tetrachloroaluminate $[C_7H_{10}S_3N_3][AlCl_4]$

Allen Applett,<sup>†</sup> Tristram Chivers,<sup>\*,†</sup> A. Wallace Cordes,<sup>\*,†</sup> and Rainer Vollmerhaus<sup>†</sup>

Received October 4, 1990

The treatment of  $(NSCl)_3$  with an excess of norbornene in dioxane at 0 °C produces  $C_7H_{10}S_3N_3Cl$  (**1**). The addition of  $AlCl_3$  or  $AgAsF_6$  to a solution of this adduct in  $SO_2$  yields  $[C_7H_{10}S_3N_3]X$  [**2a**,  $X^- = AlCl_4^-$ ; **2b**,  $X^- = AsF_6^-$ ]. The  $^{14}N$  NMR spectra of **2a**, **2b**, and  $[S_3N_3Cl]AlCl_4$  are reported. The norbornene ligand was shown by X-ray crystallography to be attached to the  $S_3N_3^+$  cation in **2a** via two sulfur atoms to give the *exo*- $\beta$  isomer. The crystals of **2a** are triclinic, space group  $P\bar{1}$ , with  $a = 7.3572$  (14) Å,  $b = 9.9771$  (15) Å,  $c = 11.1178$  (12) Å,  $\alpha = 71.561$  (11)°,  $\beta = 85.320$  (13)°,  $\gamma = 80.133$  (14)°,  $V = 762.4$  (3) Å<sup>3</sup>, and  $Z = 2$ . The least-squares refinement with anisotropic thermal parameters for all non-hydrogen atoms converged at  $R = 0.029$  and  $R_w = 0.035$  for 2686 unique observed reflections. There are pronounced variations in the sulfur-nitrogen bond lengths in the  $S_3N_3$  ring indicative of a structural weakness. The  $-N=S=N-$  unit [ $d(S-N) = 1.549$  (3) Å] is linked to the three-coordinate sulfur atoms of the SNS moiety [ $d(S-N) = 1.627$  (3) Å] by long S-N bonds [ $d(S-N) = 1.709$  (3) Å]. Attempts to detach norbornene from the  $S_3N_3$  ring in **2a** by heating or treatment with 2,3-dimethyl-1,4-butadiene resulted in loss of the  $-N=S=N-$  bridge to give the 2:1 adduct of norbornene and  $NS_2^+$ .

### Introduction

The  $S_3N_3^+$  cation is conspicuous by its absence from the list of known monocyclic, binary sulfur-nitrogen (S-N) cations, which includes examples of five-, seven-, eight-, and ten-membered ring systems [ $(S_3N_2^{++})_2$ ,  $S_4N_3^+$ ,  $S_4N_4^{2+}$ ,  $S_5N_5^+$ , respectively].<sup>1</sup> As

an example of an antiaromatic 8- $\pi$ -electron system, the molecular and electronic structures of  $S_3N_3^+$  are of interest. Assuming  $D_{3h}$  symmetry, the monomeric cation is predicted to be a triplet, and thus highly reactive, on the basis of ab initio molecular orbital calculations.<sup>2</sup> Therefore, a distorted or associated structure is

<sup>†</sup>The University of Calgary.

<sup>†</sup>University of Arkansas.

(1) Chivers, T. *The Chemistry of Inorganic Homo- and Heterocycles*; Haiduc, I., Sowerby, D. B., Eds.; Academic Press: London, 1987; Vol. 2, Chapter 29, pp 806-812.